First Order Modeling of Thermal Actuators in SUGAR

Qing Ji and Karen L. Scott

Department of Electrical Engineering and Computer Sciences,
University of California, Berkeley, CA 94720

INTRODUCTION

Electrostatic actuators have been extensively studied and have found many applications due to their low power and high frequency. Their wide use has stimulated the creation of many simulation packages used to characterize and fine-tune a design before fabrication. Designing thermal actuators is also of interest in the MEMS community because unlike electrostatic actuators, they do not require high voltages to achieve large deflections. However, the design and simulation tools available are lacking. Current simulation packages are typically based on finite element analysis, which can yield fairly accurate results but are costly and time consuming. Thermal actuators can also be modeled in SUGAR, "a simulation tool for MEMS devices based on nodal analysis techniques from the world of integrated circuit simulation. Beams, electrostatic gaps, circuit elements, etc. are modeled by small, coupled systems of differential equations".[1] SUGAR is more efficient than finite element analysis and can be used to find a quick approximate solution, which can be very valuable to a designer.

Much work has been done in modeling and experimentally characterizing thermal actuators.[2-10] The motivation of this effort is to review the existing material available in literature and derive some general equations to describe the behavior, which will also be used for modeling thermal actuators with different geometries. These general equations are implemented in SUGAR and tested for a variety of structures. The fundamental building block is a single beam characterized with first order thermal properties.

FIRST ORDER ANALYSIS OF A SINGLE BEAM UNDER HEAT

The representation of a single beam thermal actuator can be simplified for analysis using a one-dimensional problem to find the forces generated. For a single beam, when the temperature is different from the ambient temperature, it undergoes either expansion or compression. The change of the beam length can be calculated using:

$$\Delta L = \int_0^L a(T)T(x)dx\,, \qquad (1)$$

where $\alpha(T)$ is the thermal expansion coefficient. If we assume $\alpha(T)$ is a constant for various temperatures, the equation of thermal expansion can be simplified as:

$$\Delta L = a\int_0^L T(x)dx\,. \qquad (2)$$

Applying a voltage across the beam induces thermal expansion when current passes through the beam. The electrical energy will be converted to thermal energy at a rate given by:

$$E'_{thermal} = I^2 R \quad \text{(W)},$$

where I (A) is the current and R (Ω) is the electrical resistance of the beam.

In order to find the change in beam length and the force generated it is necessary to find the temperature distribution within the beam, which can be described using the following equation:

$$k\frac{d^2T}{dx^2} + J^2 r = 0 \qquad (3)$$

where J is the current density, ρ is the resistivity of the beam, and k is the thermal conductivity (W/m-Kelvin). Both resistivity ρ and thermal conductiivity k change with temperature. Assuming k is a constant and the resistivity of the beam changes linearly as the temperature varies, then k is taken equal to the value when evaluated at room temperature and

$$r = r_0\left[1 + l(T - T_s)\right] \qquad (4)$$

where ρ_0 is the resistivity at T_s and λ is the linear temperature coefficient. If we also assume $\lambda(T\text{-}T_s) << 1$, then the Eqn. (3) can be written as the following:

$$k\frac{d^2T}{dx^2} + J^2 r_0\left[1 - l\left(T - T_s\right)\right] = 0 \qquad (5)$$

The solution of the above differential equation is

$$T(x) = T_s + \frac{1}{l} + be^{tx} + ce^{-tx} \qquad (6)$$

where $t = J\sqrt{\frac{l r_0}{k}}$. b and c are constants and can be determined by boundary conditions.

For the subroutine developed, N beams in series between two anchors can be simulated. The equations with appropriate boundary conditions for individual beams are the following:

$$T_1(0) = T_s + \frac{1}{l} + b_1 e^{t_1 x}\Big|_{x=0} + c_1 e^{-t_1 x}\Big|_{x=0} = T_s + \frac{1}{l} + b_1 + c_1 = T_s$$

$$T_N(L_N) = T_s + \frac{1}{l} + b_N e^{t_N x}\Big|_{x=L_N} + c_N e^{-t_N x}\Big|_{x=L_N}$$

$$= T_s + \frac{1}{l} + b_N e^{t_N L_N} + C_N e^{-t_N L_N} = T_s$$

$$T_i(L_i) = T_s + \frac{1}{l} + b_i e^{t_i L_i} + C_i e^{-t_i L_i} = T_{i+1}(0) = T_s + \frac{1}{l} + b_{i+1} + c_{i+1}$$

$$T_i'(L_i) = b_i t_i e^{t_i L_i} - C_i t_i e^{-t_i L_i} = T_{i+1}'(0) = b_{i+1} t_{i+1} - c_{i+1} t_{i+1}$$

A matrix, shown below, is created using these equations, and the constants are found such that the temperature distribution is known in each beam.

$$\left(\begin{array}{cccccc|cccccc}
1 & 0 & 0 & \cdots & \cdots & 0 & 1 & 0 & \cdots & \cdots & \cdots & 0 \\
e^{\tau_1 L_1} & -1 & 0 & \ddots & \ddots & \vdots & e^{-\tau_1 L_1} & -1 & \ddots & \ddots & \ddots & \vdots \\
0 & e^{\tau_2 L_2} & \ddots & \ddots & \ddots & \vdots & 0 & e^{-\tau_2 L_2} & -1 & \ddots & \ddots & \vdots \\
\vdots & \ddots & \ddots & \ddots & \ddots & 0 & \vdots & \ddots & \ddots & \ddots & \ddots & \vdots \\
\vdots & \vdots & \ddots & \ddots & -1 & 0 & 0 & \cdots & \ddots & \ddots & \ddots & 0 \\
0 & \cdots & \cdots & 0 & e^{\tau_{N-1} L_{N-1}} & -1 & 0 & \cdots & \cdots & 0 & e^{-\tau_{N-1} L_{N-1}} & -1 \\
\hline
0 & \cdots & \cdots & \cdots & 0 & e^{\tau_N L_N} & 0 & 0 & \cdots & \cdots & 0 & e^{-\tau_N L_N} \\
J_1 e^{\tau_1 L_1} & -J_2 & 0 & \ddots & \ddots & \vdots & -J_1 e^{-\tau_1 L_1} & J_2 & 0 & 0 & \ddots & \vdots \\
0 & J_2 e^{\tau_2 L_2} & -J_3 & \ddots & \ddots & \vdots & \vdots & -J_2 e^{-\tau_2 L_2} & J_3 & \ddots & \ddots & \vdots \\
\vdots & \ddots & \ddots & \ddots & \ddots & \vdots & \vdots & \ddots & \ddots & \ddots & \ddots & 0 \\
\vdots & \ddots & \ddots & \ddots & \ddots & 0 & \vdots & \ddots & \ddots & \ddots & 0 & 0 \\
0 & \cdots & \cdots & 0 & J_{N-1} e^{\tau_{N-1} L_{N-1}} & -J_N & 0 & \cdots & \cdots & \cdots & -J_{N-1} e^{-\tau_{N-1} L_{N-1}} & -J_N
\end{array}\right)
\left(\begin{array}{c} b1 \\ b_2 \\ \vdots \\ \vdots \\ b_{N-1} \\ b_N \\ c_1 \\ c_2 \\ \vdots \\ \vdots \\ c_{N-1} \\ c_N \end{array}\right)
=
\left(\begin{array}{c} 1/\lambda \\ 0 \\ \vdots \\ \vdots \\ 0 \\ 1/\lambda \\ 0 \\ 0 \\ \vdots \\ \vdots \\ \vdots \\ 0 \end{array}\right)$$

Once the temperature distribution for each beam is known, ΔL and an equivalent force generated due to thermal expansion can be found using the following equation.

$$F = AE\frac{\Delta L}{L}$$

These equations represent a first order approximation for the beam expansion, temperature distribution, and force generated for a single beam[5-7], which were implemented to create a net list that can be solved using SUGAR.

SUGAR IMPLEMENTATION

A new subroutine "cho_therm('*netlist*')" was created, which reads in a SUGAR net list, calculates the forces generated due to thermal expansion, and creates a modified net list with appropriate forces appended. The source code for the thermal subroutine can be found at:
http://www-bsac.EECS.Berkeley.EDU/~klscott/.

Inside the subroutine, the geometry of the structure is determined to find the total resistance and the current density in each beam. Once the current density is known, the above mentioned matrix equation is solved to determine the temperature distribution in each beam, which is then used to calculate the change in length of the beam due to thermal expansion and the corresponding force generated. A new net list is written consisting of the original beams and appended with the appropriate forces that were generated. For a beam attached to an anchor, the full force is applied to the non-anchored end. For a beam attached to two other beams, half the total force is applied at each node and in the appropriate directions.

The new net list can then be processed using the standard SUGAR routines, which will determine the final geometry of the structure. When SUGAR is executed, it also outputs the temperature at each node. A basic SUGAR net list and the modified net list using "cho_therm", used to characterize the Guckel thermal actuator, are as follows.

Guckel.net:
```
% A simple SUGAR netlist
% used to describe a Guckel thermal actuator.

uses mumps.net

Vsrc    *  [a e] [V=5.8971]
eground  *  [e]   []
anchor p1 [a] [l=6u w=6u h=2u]
beam3d p1 [a b] [l=312u w=2u oz=0 h=2u]
beam3d p1 [b c] [l=2u w=5u oz=pi/2 h=2u]
beam3d p1 [c d] [l=250u w=15u oz=-pi h=2u]
beam3d p1 [d e] [l=62.5u w=2u oz=-pi h=2u]
anchor p1 [e]   [l=6u w=6u h=2u]
```

NewGuckel.net:
uses mumps.net

```
anchor p1 [a] [l=6u w=6u h=2u]
beam3d p1 [a b] [l=312u w=2u oz=0 h=2u]
f3d  * [b] [F=899.6979u oz=0]
beam3d p1 [b c] [l=2u w=5u oz=pi/2 h=2u]
f3d  * [c] [F=1329.4324u oz=pi/2]
f3d  * [b] [F=-1329.4324u oz=pi/2]
beam3d p1 [c d] [l=250u w=15u oz=-pi h=2u]
f3d  * [d] [F=2698.9105u oz=-pi]
f3d  * [c] [F=-2698.9105u oz=-pi]
beam3d p1 [d e] [l=62.5u w=2u oz=-pi h=2u]
f3d  * [d] [F=-215.2996u oz=-pi]
anchor p1 [e]   [l=6u w=6u h=2u]
```

Ideally the thermal subroutine should be encapsulated within a model function and the forces generated should be added appropriately to the global equation. Due to time constraints we were more concerned with understanding and being able to explain our results.

There are a few caveats worth mentioning. The subroutine is not as robust as the standard I/O routines written for SUGAR and has the following limitations; there are no defaults or checks for values that are missing, all units are defaulted to microns, resistivity and thermal expansion values are variables rather than input parameters, nodes can be named only with one letter, beams can only have one angle associated with them, and the new file is created in a set home directory.

There is also a caveat worth mentioning in regards to SUGAR, because it can be an issue for correct modeling of thermal actuators. SUGAR does its calculations based on a beam model, which is accurate for beams with an aspect ratio greater than ten. If a beam has an aspect ratio less than ten, there is code that has been written which utilizes a plate model as opposed to a beam model. The user should use the appropriate code for the problem.

RESULTS AND DISCUSSION

Both Chevron and Guckel thermal actuators were modeled using the subroutine "cho_therm('net')". A simple Chevron thermal actuator is shown in Figure 1. Actuators with various lengths, widths, heights, and pre-angles α have been simulated at different voltage biases. Table 1 gives the dimensions of the Chevron thermal actuators used for the simulations. The simulation results using SUGAR are compared to other experimental data from Que et al[8] and Sinclair et al[9], as shown in Figure 2. The simulated tip deflections are generally higher than the experimental results. Most of the simulated results are within a factor of two of the experimental results. At low voltage in Fig 2(a), the ratio of

simulated results to experimental data can be as high as approximately four.

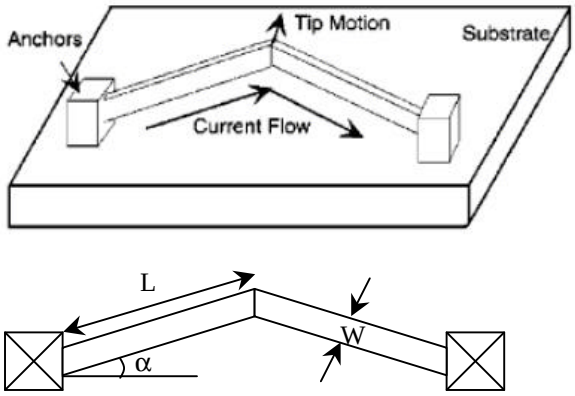

Figure 1. Schematic of a chevron bent-beam thermal actuator (taken from reference 7).

Table 1. The length, width, height, and pre-angle of Chevron thermal actuators used in simulations and experiments.

	Q1[8]	Q2[8]	Q3[8]	Q4[8]	S1[9]	S2[9]	S3[9]
L (μm)	800	800	800	800	200	200	200
W (μm)	13.9	13.9	13.9	13.9	2.0	2.0	2.0
H (μm)	3.7	4.75	4.75	3.37	2.0	2.0	2.0
α (mrad)	200	100	200	200	9.1	22.9	38.0

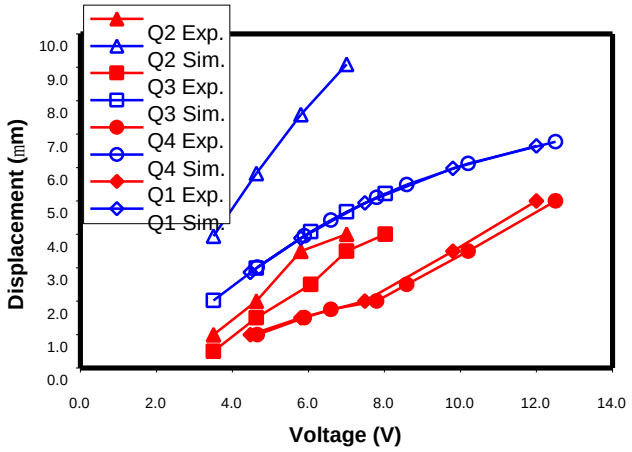

(a)

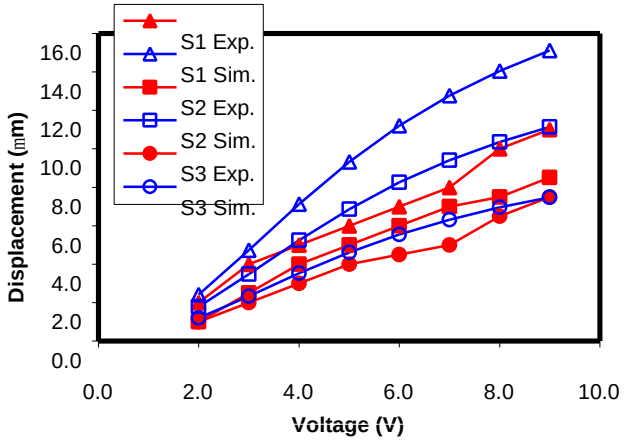

(b)

Figure 2. Comparison of tip deflection of Chevron thermal actuators simulated by SUGAR and corresponding experiment results of (a) Que et al[8] and (b) Sinclair et al[9].

A simple Guckel thermal actuator is shown in Figure 3. Actuators with various arm lengths, widths and heights have been simulated at different voltage biases. Tables 2 gives the dimensions of the Guckel thermal actuators used for the simulations. The simulation results using SUGAR are compared to other experimental data from Huang et al[7] and Kolesarr et al[11], as shown in Figure 4. In Fig. 4(a), when compared to data taken by Kolesar et al, the simulation overestimates the tip deflection, which is similar to the case of Chevron thermal actuator. Poor correlation was found at low bias voltages, the simulated tip deflection could be as high as ten times of the experimental data. In Fig. 4(b), agreement was very good for the experimental data taken by Huang, except some of the simulated results are below a factor of two with respect to the experimental results.

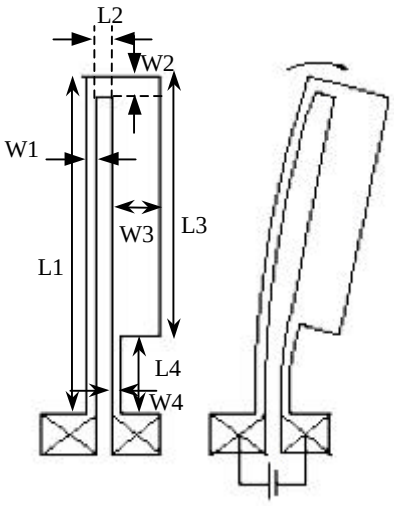

Figure 3. Schematic of a Guckel thermal actuator (taken from reference 4).

Table 2. The lengths, widths, and heights of each section of the Guckel thermal actuators used in simulations and experiments.

	K1[11]	H1[7]	H2[7]	H3[7]
L1 (μm)	312.5	240	240.0	240.0
W1 (μm)	2.0	3.0	4.0	3.0
H1 (μm)	2.0	2.0	2.0	2.0
L2 (μm)	2.0	2.5	2.5	2.5
W2 (μm)	5.0	5.0	5.0	5.0
H2 (μm)	2.0	2.0	2.0	2.0
L3 (μm)	250.0	180.0	180.0	120.0
W3 (μm)	15.0	12.0	12.0	12.0
H3 (μm)	2.0	2.0	2.0	2.0
L4 (μm)	62.5	60.0	60.0	120.0
W4 (μm)	2.0	3.0	4.0	3.0
H4 (μm)	2.0	2.0	2.0	2.0

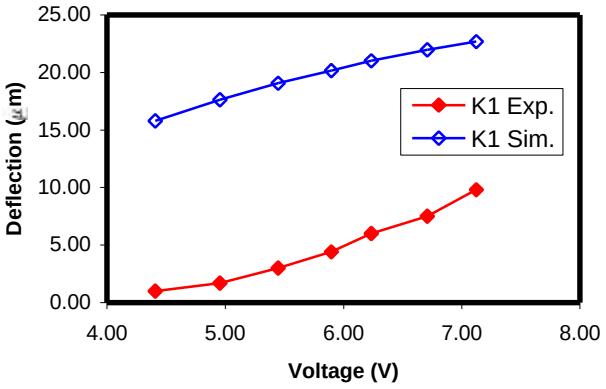

(a)

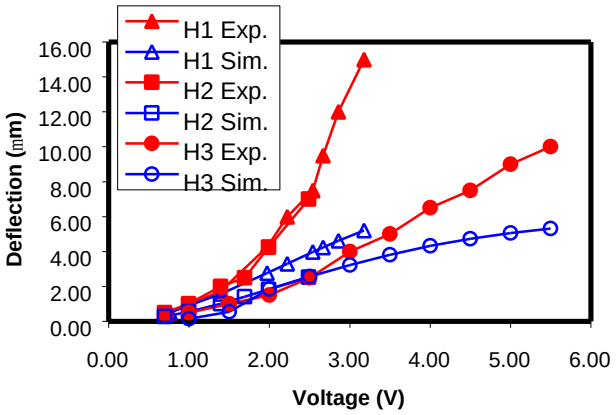

(b)

Figure 4. Comparison of tip deflection of a Guckel thermal actuators simulated by SUGAR and corresponding experimental results of (a) Kolesar et al[11] and (b) Huang et al[7].

The assumption of $\lambda(T-T_s) << 1$ used in order to obtain a closed form description of temperature distribution within the beams is only valid when $\Delta T << 1/\lambda$. The hotest spot of the beams should be lower than $T_s+1/\lambda = 1027$ °C. The highest temperature for each simulation case, shown in Table 3, is 950 °C. Therefore, the approximation still holds for all the simulations above.

Table 3. Maximum beam tip temperatures.

Chevron	**Q1**[8]	**Q2**[8]	**Q3**[8]	**Q4**[8]	**S1**[9]**, S2**[9]**, S3**[9]
T (°C)	939	711	782	950	882
Guckel	**K1**[11]	**H1**[7]	**H2**[7]	**H3**[7]	
T (°C)	771	502	369	789	

In this first order one-dimensional modeling, heat loss from the beam such as radiation to the atmosphere and substrate through air is neglected. This could explain the overestimation of the tip deflection compared to the experimental data. Additional errors are generated because the thermal conductivity k and the thermal expansion coefficient α of the material are not constant as temperature varies.

CONCLUSION

A first order model for thermal actuators has been implemented in SUGAR. Even though no heat loss effects were considered, the general trends and behaviors are predicted fairly well. Parasitic heat loss and the non-linear effects of the thermal conductivity k and the thermal expansion coefficient α will need to be accounted for to increase the accuracy between the model and the experimental results.

REFERENCES

[1] Sugar: www-bsac.eecs.Berkeley.edu/~cfm

[2] Guckel H, Klein J, Christenson T, Skrobis K, Laudon M, and Lovell EG, "Thermo-magnetic metal flexure actuators", Technical Digest, 1992 Solid State Sensors and Actuators Workshop (Hilton Head, SC, USA) (1992) 73-5.

[3] Comtois JH, Michalicek MA, Barron CG, "Electrothermal actuators fabricated in four-level planarized surface micromachined polycrystalline silicon", Sensors and Actuators A **70** (1998) 23-31.

[4] Reid JR, Bright VM, Comtois JH, "Force measurements of polysilicon thermal microactuators", Proceedings of the SPIE (Micromachined Devices and Components II) **2882** (1996) 296-306.

[5] Mankame ND, Ananthasuresh GK, "Comprehensive thermal modelling and characterization of an electro-thermal-compliant microactuator", J. Micromech. Microeng. **11** (2001) 452-462.

[6] Judy J.W., Tamagawa, T. and Polla D.L., "Surface Micromachined Linear Thermal Microactuator", IEDM (1990) 629.

[7] Huang, Q.-A. and Lee N.K.S., "Analytical modeling and optimization for a laterally-driven polysilicon thermal actuator", Microsystem Technologies, 5 (1999) 133-137.

[8] Que L, Park JS, Gianchandani YB, "Bent-Beam Electrothermal Actuators – Part I: Single Beam and Cascaded Devices", JMEMS **10**-2, (2001) 247-254.

[9] M.J. Sinclair, "A High Force Low Area MEMS Thermal Actuator", Inter Society Conference on Thermal Phenomena (2000) 127-132.

[10] J.-S. Park, L.L. Chu, E. Siwapornsathain, A.D. Oliver, Y.B. Gianchandani, "Long Throw and Rotary Output Electro-Thermal Actuators Based on Bent-Beam Suspensions", Proceedings IEEE Thirteenth Annual International Conference on MEMS (1999) 680-685.

[11] E. S. Kolesar, S. Y. Ko, J. T. Howard, P. B. Allen, J. M. Wilken, N. C. Boydston, M. D. Ruff and R. J. Wilds, " In-plane tip deflection and force achieved with asymmetrical polysilicon electrothermal microactuators", Thin Solid Films (2000) 719-726.